

## Hydrophilic and Lipophilic Iron Chelators with the Same Complexing Abilities

Daniel Imbert, Paul Baret, Didier Gaude, Isabelle Gautier-Luneau, Gisèle Gellon, Fabrice Thomas, Guy Serratrice, and Jean-Louis Pierre\*<sup>[a]</sup>

**Abstract:** A new series of iron chelators with the same coordination sphere as the water-soluble ligand O-trensox, but featuring a variable hydrophilic–lipophilic balance, have been obtained by grafting oxyethylene chains of variable length on a C-pivot tripodal scaffold. The X-ray structure of a ferric complex exhibiting tris(8-hydroxyquinolate) coordination and solution thermodynamic properties ( $pK_a$  of the ligands, stability constants of

the ferric complexes) have been determined. The complexing ability ( $pFe^{III}$  values) of the ligands are similar to that of O-trensox. Partition coefficients between water and octanol or chloroform have been measured and transport

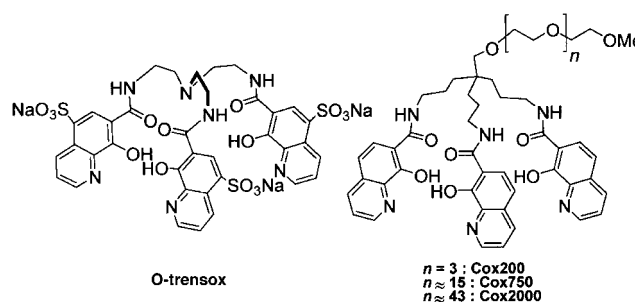
**Keywords:** chelates • iron • lipophilicity • partition coefficients • tripodal ligands

across a membrane has been mimicked (“shuttle process”). The results of biological assays (iron chelation with free ligands or iron nutrition with ferric complexes) could not be correlated with the partition coefficients. These results call into question the role of distribution coefficients (of the ligands and/or complexes) in the biological activities of iron chelators.

### Introduction

Iron chelation by natural or abiotic chelators can be applied to human diseases caused by iron overload, and iron complexes of similar chelators can be used to alleviate iron deficiency in plants, preventing and even reversing iron chlorosis.<sup>[1]</sup> The ability of the chelator to fulfil these functions is related primarily to its powerful and selective affinity for the metal, revealed by the  $pFe^{III}$  value.<sup>[2]</sup> Water solubility is required, but it is generally claimed that access to the cell through biological membranes depends on the lipophilicity of the chelator or of its iron complex. This lipophilicity is usually measured in terms of the partition coefficient  $P$  between  $n$ -octanol and water or, less often, between chloroform and water.<sup>[3]</sup> Other factors affecting a compound's ability to permeate liquid membranes freely are molecular weight, size and ionisation.

We have developed the efficient water-soluble chelator O-trensox<sup>[4,5]</sup>, which exhibits a strong complexing ability for ferric iron ( $pFe^{III} = 29.5$ ) and a high selectivity towards its complexation compared with other biological metal ions ( $pCu^{II} = 22.8$ ,  $pZn^{II} = 21.7$ ,  $pFe^{II} = 17.9$ ,  $pCa^{II} = 13.6$ ).<sup>[6]</sup> The octanol/water partition coefficients of O-trensox (0.02) and of



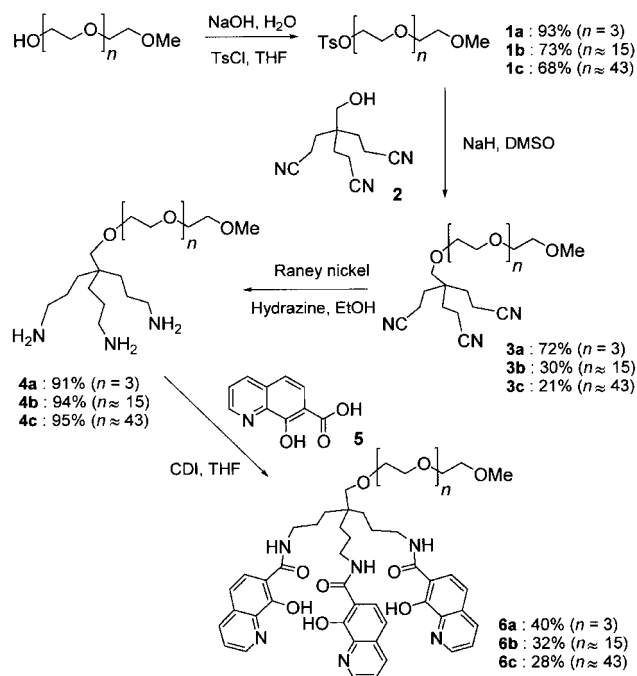
its iron complex ( $<0.005$ ) show the insolubility of these species in octanol.<sup>[7]</sup> Moreover, the molecular mass of O-trensox is too high for it to use membrane aquaporin channels, so O-trensox and its iron complex would not be expected to exhibit biological activity requiring them to cross cell membranes. Nevertheless, cellular protection is obtained with O-trensox through iron mobilisation from rat hepatocytes in vitro and in vivo,<sup>[8]</sup> and the ferric complex of O-trensox enables plant cells to metabolise iron.<sup>[9]</sup> These surprising results led us to imagine a series of iron chelators with the same coordination sphere as O-trensox (similar  $pFe^{III}$  values), but a variable hydrophilic–lipophilic balance, modulated by a polyoxyethylenic chain of variable length grafted on a C-pivot tripodal scaffold. Short-chain polyether analogues of DFO (desferrioxamine) with enhanced lipophilicity, but still water-soluble, have been evaluated for chelating iron in rats.<sup>[10]</sup>

[a] J.-L. Pierre, D. Imbert, P. Baret, D. Gaude, I. Gautier-Luneau, G. Gellon, F. Thomas, G. Serratrice  
Laboratoire de Chimie Biomimétique, LEDSS  
UMR CNRS 5616, Université Joseph Fourier  
BP 53, 38041 Grenoble Cedex 9 (France)  
Fax: (+33)4-76-51-48-36  
E-mail: jean-louis.pierre@ujf-grenoble.fr

Here we describe the synthesis of the ligands and of their iron complexes, and we try to correlate their physicochemical properties, including their structural characterisation, solution thermodynamics and liquid membrane transport, with biological activities.

## Results and Discussion

**Syntheses:** We have described the C-pivot tripodal starting compound **2** previously.<sup>[11]</sup> The poly(oxyethylene) (POE) chains were grafted onto the tripodal template by using the Williamson's method, then the cyano functions of **3** were reduced to give the triamine **4**, which in the last step reacted with 7-carboxy-8-hydroxyquinoline **6** activated by carbonyldiimidazole (Scheme 1). The products **6b** (Cox750) and **6c** (Cox2000) are polymeric materials, whereas the polyether chain has a defined length in **6a** (Cox200).



Scheme 1. Ligand syntheses.

**Iron complexes:** The iron(III) complex of Cox200 was obtained by adding three equivalents of KOH and one equivalent of  $[\text{Fe}(\text{acac})_3]$  to a solution of the ligand in degassed methanol/dichloromethane. The complex was purified by standard procedures. The 1:1 stoichiometry was demonstrated by FAB<sup>+</sup> mass spectroscopy ( $m/z$  for  $[\text{L} - 3\text{H} + \text{Fe}]^+$ ; L = ligand). The 8-hydroxyquinolate bonding mode (coordination with the nitrogen and the oxygen atoms) was established unambiguously from the X-ray structural determination of the Cox200 ferric complex (vide infra). The 1:1 stoichiometry of Cox750 and Cox2000 was demonstrated by UV/Vis spectroscopy (Job's method) in a pH 7.4 buffered aqueous solution.<sup>[12]</sup> The aqueous solutions of the complexes exhibit similar spectra with main features at 450 ( $\epsilon = 4600 \text{ M}^{-1} \text{ cm}^{-1}$ ) and 590 nm ( $\epsilon = 3900 \text{ M}^{-1} \text{ cm}^{-1}$ ) attributed to phenolate–Fe and pyridine–Fe

LMCT transitions, respectively. These data reveal a tris-(8-hydroxyquinolate) type of complexation, like that previously demonstrated for the ferric complex of O-trensox.<sup>[5]</sup>

**X-ray structure of Fe–Cox200:** Single crystals of the Fe–Cox200 complex  $[\text{Fe}(\text{C}_{50}\text{H}_{57}\text{N}_6\text{O}_{11})] \cdot \text{H}_2\text{O}$  were obtained by diffusion of diethyl ether into a solution of the complex in methanol. Its crystal structure reveals a neutral mono-iron(III) complex with a distorted octahedral tris(8-hydroxyquinolate) coordination geometry for Fe<sup>III</sup>.

The  $\text{N}_3\text{O}_3$  iron-coordination sphere is provided by the three 8-hydroxyquinoline arms of the ligand (all the atoms of each arm connected to the tripodal carbon spacer C14 are labelled a, b or c) (Figure 1). Each 8-hydroxyquinoline subunit forms a five-membered chelate ring with iron, leading to the facial isomer. Selected bond lengths and angles are given in Table 1. The average five-membered chelate ring O1x–Fe–N1x angle ( $x = a, b$  or  $c$ ) is  $78.6^\circ$  and is close to that observed for the

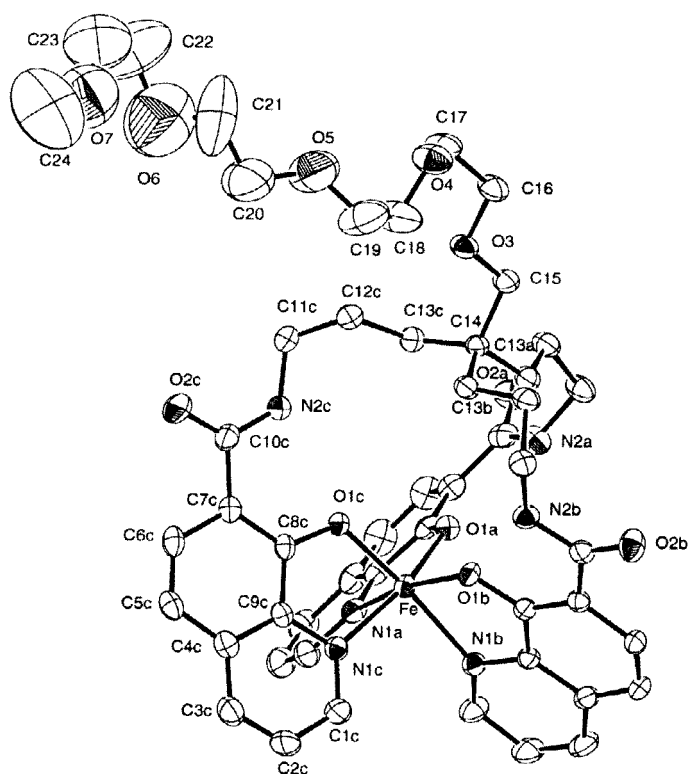


Figure 1. ORTEP plot of Fe–Cox200. Hydrogen atoms are omitted for clarity. Ellipsoids are drawn at the 30% probability level.

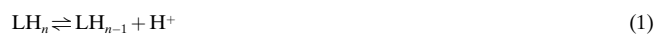
Table 1. Selected bond lengths [ $\text{\AA}$ ] and angles [ $^\circ$ ] for Fe–Cox200.

Fe–O1a	1.949(3)	Fe–N1a	2.184(4)
Fe–O1b	1.935(3)	Fe–N1b	2.166(4)
Fe–O1c	1.959(3)	Fe–N1c	2.143(4)
O1a–Fe–N1a	78.5(1)	O1a–Fe–N1c	164.2(1)
O1b–Fe–N1b	78.9(1)	O1b–Fe–N1a	165.2(1)
O1c–Fe–N1c	78.6(1)	O1c–Fe–N1b	171.1(1)
O1b–Fe–O1a	95.4(1)	N1b–Fe–N1a	88.0(1)
O1b–Fe–O1c	98.3(1)	N1c–Fe–N1b	93.5(1)
O1a–Fe–O1c	95.6(1)	N1c–Fe–N1a	87.4(1)
O1a–Fe–N1b	93.1(1)	O1b–Fe–N1c	100.0(1)
O1c–Fe–N1a	95.7(1)		

tris(8-hydroxyquinolato)iron(III) complex (79.2°),<sup>[13]</sup> whereas all *cis* angles are in the range 87.4(1)°–100.0(1)° and apical angles are in the range 164.2(1)°–171.1(1)°. The three 8-hydroxyquinoline groups (O1*x*, N1*x*, C1*x*–C9*x*, *x* = a, b or c) are planar with a maximum mean deviation of plane c of 0.018 Å. The dihedral angles between the planes a, b and c are 91.24° (a–b), 90.28° (a–c) and 71.25° (b–c). The three arms are long enough to allow nonrestricting complexation around the iron metal. The bond lengths with iron(III) are in narrow ranges: between 1.935(3) and 1.959(3) Å for Fe<sup>III</sup>–O and between 2.143(4) and 2.184(4) Å for Fe<sup>III</sup>–N bonds. These are very close to the bond lengths observed in the tris(8-hydroxyquinolato)iron(III) complex with *mer* geometry,<sup>[13]</sup> in which the Fe–N bond lengths lie between 2.125(6) and 2.172(5) Å, and two of the Fe–O bonds are similar in length (1.936(5) and 1.956(5) Å), while the third is longer (1.996(5) Å). The difference could be explained by the *mer* geometry of this complex. The Fe–O bond lengths may also be compared with the average Fe–O (hydroxyl oxygen) bond lengths in the tris(salicylate) complexes, 1.94 Å for [Fe(O-trensox)]<sup>[14]</sup> and 1.92 Å for [Fe(trensam)] and [Fe(tren(3M)-sam)]<sup>[15]</sup> (trensam = tris[(2-hydroxybenzoyl)-2-aminoethyl]amine; tren(3M)sam = tris[(2-benzyloxy-3-methoxybenzoyl)-2-aminoethyl]amine) and in the tris(catecholate), 2.01 Å for [Fe(trencam)] (trenca = tris[(2,3-dihydroxybenzoyl)-2-aminoethyl]amine). To our knowledge this is the first example of a Fe<sup>III</sup> complex structure with 1:1 stoichiometry exhibiting *fac* tris(8-hydroxyquinolato) coordination. Only the Fe<sup>III</sup> complex with O-trensox, obtained in an acidic medium and involving tris(salicylate)-type coordination, has been described.<sup>[7]</sup> Furthermore, the structure reveals that amide protons interact strongly by hydrogen bonding with the quinolinol oxygen coordinated to iron forming three six-membered rings. The H2*nx*⋯O1*x* and the N2*x*⋯O1*x* distances (*x* = a, b or c) are 1.83, 1.86, 2.04 Å and 2.677, 2.672, 2.713 Å, respectively. Hydrogen bonding between the amide hydrogen and the *ortho* quinolinol oxygen is an important feature of the structure and is claimed to enhance the stability of the complex. This interaction is also observed in iron triscatecholate and other complexes with this type of ligand. For [Fe(trencam)] the NH⋯O distances vary from 1.80 to 1.85 Å.<sup>[16]</sup>

**Thermodynamic solution studies:** These studies were performed as described previously for O-trensox.<sup>[5]</sup> Here we present the results for the water-soluble ligand Cox2000.

**Ligand deprotonation constants:** The fully protonated form of Cox2000 possesses six deprotonation sites (three pyridinium nitrogen and three hydroxyl oxygen atoms) and is denoted LH<sub>6</sub><sup>3+</sup>. The potentiometric titration of the fully protonated ligand with NaOH in 0.1 M NaClO<sub>4</sub> at 25 °C (Figure 2, curve a) allowed the determination of five deprotonation constants. Analysis of the potentiometric titration curve over the pH range 2.5–10.5 by the SUPERQUAD<sup>[17]</sup> program yielded the p*K*'<sub>*a*<sub>*n*</sub></sub> values (127 points, σ<sub>fit</sub> = 3.7) defined by Equations (1) and (2).



$$K_{a_n} = \frac{[\text{LH}_{n-1}][\text{H}^+]}{[\text{LH}_n]} \quad (2)$$

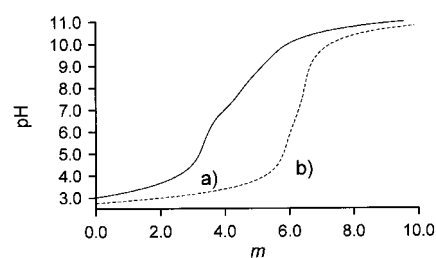


Figure 2. Potentiometric titration curves for a) ligand Cox2000 (1 mM); b) Cox2000 (1 mM) + Fe<sup>III</sup> (1 mM); *m* = mol base added per mol ligand, *T* = 25 °C, *I* = 0.1 M (NaClO<sub>4</sub>).

Hence p*K*'<sub>*a*<sub>5</sub></sub> = 2.89 ± 0.02, p*K*'<sub>*a*<sub>4</sub></sub> = 4.13 ± 0.02, p*K*'<sub>*a*<sub>3</sub></sub> = 6.80 ± 0.02, p*K*'<sub>*a*<sub>2</sub></sub> = 8.40 ± 0.01, p*K*'<sub>*a*<sub>1</sub></sub> = 10.38 ± 0.01, but the lowest p*K*'<sub>*a*<sub>*n*</sub></sub> values cannot be determined from this analysis.

A spectrophotometric titration was carried out over the pH range 1–11 (Figure 3). First, the absorbance data of the UV spectra in the pH range 1.02–4.78 (Figure 3A) were processed by the nonlinear least-squares program LETAGROP-SPEFO<sup>[18, 19]</sup> (absorbance values at nine wavelengths between

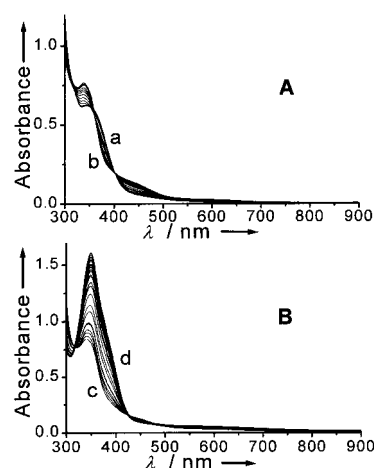


Figure 3. UV/Vis absorption spectra of Cox2000 as a function of pH: [Cox2000] = 0.1 mM, *T* = 25 °C, *I* = 0.1 M (NaClO<sub>4</sub>). pH values: A) a) 1.02, b) 4.78; B) c) 6.15, d) 10.88.

320 and 480 nm). The best fit ( $\Sigma(A_{\text{exptl}} - A_{\text{calcd}})^2 = 10^{-2}$ ), obtained by considering the two deprotonation equilibria represented by Equations (3) and (4), yielded p*K*'<sub>*a*<sub>6</sub></sub> = 2.43 ± 0.15 and p*K*'<sub>*a*<sub>5</sub></sub> = 7.14 ± 0.09, respectively.



The *K*'<sub>*a*<sub>5</sub></sub> value is in good agreement with the sum p*K*'<sub>*a*<sub>5</sub></sub> + p*K*'<sub>*a*<sub>4</sub></sub> = 7.02 determined from potentiometric measurements. Second, analysis of the absorbance data over the pH range 6.15–10.88 (Figure 3B) by the LETAGROP-SPEFO program (absorbance values at 10 wavelengths between 340 and 450 nm,  $\Sigma(A_{\text{exptl}} - A_{\text{calcd}})^2 = 10^{-3}$ ) led to the equilibria of Equations (5) and (6) and yielded the values p*K*'<sub>*a*<sub>3</sub></sub> = 7.11 ± 0.19 and p*K*'<sub>*a*<sub>2</sub></sub> = 18.75 ± 0.01, respectively.



These values are in good agreement with the  $pK_{a_3}$  (6.80) and the sum  $pK_{a_2} + pK_{a_1} = 18.78$  determined from potentiometric measurements.

Compared with the  $pK_a$  values of O-trensox,<sup>[5]</sup> the three lowest  $pK_a$  values are attributed to the pyridinium nitrogen atoms and the three highest to the hydroxy moieties. The average deprotonation constants are 3.15 for the pyridinium nitrogen atoms ( $pK_{av(4-6)}$ ) and 8.53 for the hydroxy groups ( $pK_{av(1-3)}$ ). The corresponding values for O-trensox, 2.46 and 8.07, respectively, are lower because of the electron-withdrawing effect of the sulfonate groups. The  $pK_a$  ranges for the pyridinium nitrogen atoms (2.43, 2.89 and 4.13) and the hydroxy groups (6.80, 8.40 and 10.38) differ from the statistical factor of  $\log 3$  (i.e., 0.48), indicating that there is some cooperativity between the three arms of the tripod, in contrast to the situation in O-trensox.

**Stability constants of the ferric complexes:** The equilibria of the metal complexes were studied by means of potentiometric and spectrophotometric titrations. The potentiometric titration curve of a 1:1 solution of ferric ion and Cox2000 (Figure 2, curve b) shows a large jump in pH at  $m=6$ , indicating that all the ligand protons are released when the ligand binds ferric ion at pH 7.4. However, it was not possible to determine  $\log \beta_{110}$ , since formation of the complex is complete at low pH values. The spectrophotometric titration was carried out from pH 0 to pH 11 in order to determine the deprotonation constants of the ferric complex and the global constants  $\beta_{11n}$  defined by Equation (7).

$$\beta_{11n} = [\text{FeLH}_n] / [\text{Fe}^{3+}][\text{L}][\text{H}^+]^n \quad (7)$$

Between pH 0 and pH 1 (Figure 4A) a charge-transfer band appears at  $\lambda_{\text{max}} = 440$  nm with a shoulder at 550 nm. The absorbance data were refined with the program LETAGROP-SPEFO (absorbance values at 18 wavelengths between 440 and 800 nm). The best refinement ( $\sum(A_{\text{exptl}} - A_{\text{calcd}})^2 = 2 \times 10^{-2}$ ) was obtained by considering the formation of the  $\text{FeLH}_4^{4+}$  species, and provided the values  $\log \beta_{114} = 38.98 \pm 0.11$  and  $\epsilon = 4600 \text{ M}^{-1} \text{ cm}^{-1}$  at  $\lambda_{\text{max}} = 440$  nm. The value  $\log K_{\text{FeLH}_4} = 3.95 \pm 0.11$  was deduced, whereby  $K_{\text{FeLH}_4}$  is defined by Equations (8) and (9).



$$K_{\text{FeLH}_4} = [\text{FeLH}_4^{4+}][\text{H}^+]^2 / [\text{Fe}^{3+}][\text{LH}_6^{3+}] \quad (9)$$

An increase in the pH from 1 to 1.91 resulted in the appearance of a charge-transfer band at  $\lambda_{\text{max}} = 560$  nm with an isobestic point at 372 nm (Figure 4B), indicating the presence of only two species with different absorbances. These absorbance data were also refined with the LETAGROP-SPEFO program (absorbance values at 24 wavelengths between 340 and 800 nm). The best fit ( $\sum(A_{\text{exptl}} - A_{\text{calcd}})^2 = 9 \times 10^{-3}$ ) showed that deprotonation occurs in a three-proton step yielding  $\log \beta_{111} = 34.24 \pm 0.05$  and absorption maxima at  $\lambda_{\text{max}} = 440$  nm ( $\epsilon = 4600 \text{ M}^{-1} \text{ cm}^{-1}$ ) and  $\lambda_{\text{max}} = 560$  nm ( $\epsilon = 2900 \text{ M}^{-1} \text{ cm}^{-1}$ ) for the  $\text{FeLH}^+$  species. When the pH was raised from 1.91 to 3.48 (Figure 4C) an

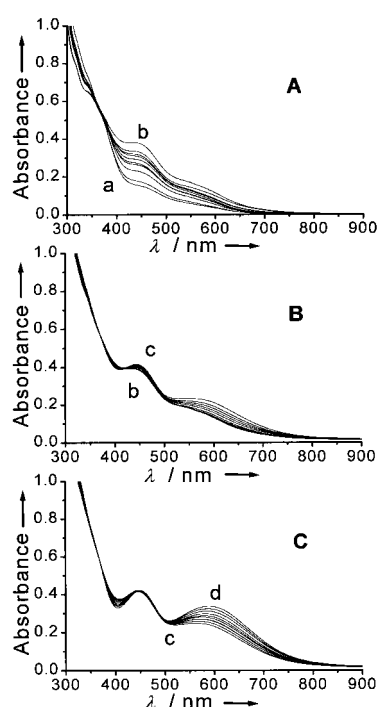


Figure 4. UV/Vis absorption spectra of  $\text{Fe}^{\text{III}}-\text{Cox2000}$  as a function of pH:  $[\text{Cox2000}] = [\text{Fe}] = 0.1 \text{ mM}$ ,  $I = 0.1 \text{ M}$  ( $\text{NaClO}_4$ ). pH values for A), B) and C): a) 0, b) 1, c) 1.91, d) 3.48.

increase in  $\lambda_{\text{max}}$  from 440 to 450 nm and from 560 to 590 nm was observed with an increase in the molar extinction coefficient. The refinement of the absorbance data with the LETAGROP-SPEFO program (absorbance values at 24 wavelengths between 340 and 800 nm,  $\sum(A_{\text{exptl}} - A_{\text{calcd}})^2 = 3 \times 10^{-2}$ ) provided  $\log \beta_{110} = 32.12 \pm 0.09$ ,  $\epsilon = 4600 \text{ M}^{-1} \text{ cm}^{-1}$  ( $\lambda_{\text{max}} = 450$  nm) and  $\epsilon = 3900 \text{ M}^{-1} \text{ cm}^{-1}$  ( $\lambda_{\text{max}} = 590$  nm) for the  $\text{FeL}$  species. No spectral change was observed until pH 9, beyond which absorbances decreased at all the wavelengths, suggesting the formation of hydroxo complexes.

The constants and spectral parameters are collected in Table 2. The value of  $\log \beta_{114}$  is less accurate than that of  $\log \beta_{111}$  and  $\log \beta_{110}$ , because the ionic strength varied over the pH range 0–1. The distribution of the species according to pH are shown in Figure 5.

Table 2. Equilibrium constants,  $\log \beta_{11n}$  and UV/Vis spectral characteristics of ferric Cox2000 complexes.

Complex	$\log \beta_{11n}$	$p\text{Fe}^{\text{III[a]}}$	$\lambda_{\text{max}}$ [nm]	$\epsilon$ [ $\text{M}^{-1} \text{ cm}^{-1}$ ]
$\text{FeLH}_4^{4+}$	$38.98 \pm 0.11$		440	4400
$\text{FeLH}^+$	$34.24 \pm 0.05$		440	4600
			560	2900
$\text{FeL}$	$32.12 \pm 0.09$	29.1	450	4600
			590	3900

[a]  $p\text{Fe}^{\text{III}} = -\log[\text{Fe}^{3+}]$ , calculated for  $[\text{Fe}^{3+}] = 10^{-3} \text{ mM}$ ,  $[\text{L}] = 10^{-2} \text{ mM}$  and  $\text{pH} = 7.4$ .

The stability constants  $\beta_{110}$  of the ferric complex  $\text{FeL}$  were also determined by spectrophotometric competition experiments with ethylenediaminetetraacetic acid (edta) over the pH range 2.05–2.49. The competition equilibrium can be

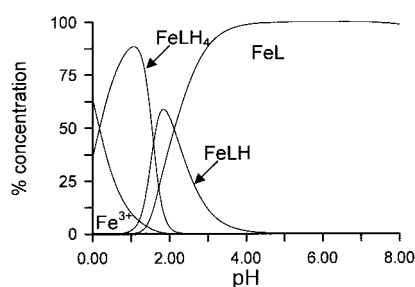


Figure 5. Distribution curves for Fe<sup>III</sup>–Cox2000 species at pH 1–8: [Cox2000] = [Fe<sup>3+</sup>] = 0.1 mM.

expressed by Equations (10) and (11), in which Y denotes edta, LH<sub>6</sub><sup>3+</sup> the ligand Cox2000, K<sub>a1</sub>–K<sub>a6</sub> the deprotonation constants of LH<sub>6</sub><sup>3+</sup> and K'<sub>a1</sub>, K'<sub>a2</sub> and K'<sub>a3</sub> the deprotonation constants of YH<sub>3</sub><sup>[20]</sup>.



$$K = \frac{[\text{FeY}][\text{LH}_6^{3+}][\text{FeL}][\text{YH}_3][\text{H}^+]^3}{\beta_{110(\text{FeY})}K_{a1}K_{a2}K_{a3}/\beta_{110(\text{FeL})}K_{a1}K_{a2}K_{a3}K_{a4}K_{a5}K_{a6}} \quad (11)$$

The concentration of FeL was calculated from the absorbance *A* at 590 nm according to Equation (12), in which *K*<sub>FeLH</sub> is the deprotonation constant of the FeLH complex.

$$A = [\text{FeL}](\epsilon_{\text{FeL}} + \epsilon_{\text{FeLH}}[\text{H}^+]/K_{\text{FeLH}}) \quad (12)$$

The concentrations of the other species in Equations (10) and (11) were calculated from the mass balance equation and pH [Eqs. (13)–(15), in which each *α* is the usual Ringbom coefficient].<sup>[21]</sup>

$$[\text{Fe}]_{\text{tot}} = \alpha_{\text{FeL}}[\text{FeL}] + \alpha_{\text{FeY}}[\text{FeY}] \quad (13)$$

$$[\text{L}]_{\text{tot}} = \alpha_{\text{FeL}}[\text{FeL}] + \alpha_{\text{L}}[\text{L}] \quad (14)$$

$$[\text{Y}]_{\text{tot}} = \alpha_{\text{FeY}}[\text{FeY}] + \alpha_{\text{Y}}[\text{Y}] \quad (15)$$

From the known formation constant of FeY (log β<sub>110</sub> = 25.0),<sup>[20]</sup> an average formation constant obtained for the ferric Cox2000 complex (log β<sub>110</sub> = 32.3) is in good agreement with that (32.1) determined from the spectrophotometric titration.

The visible spectrum of the FeLH<sub>4</sub><sup>4+</sup> species (λ<sub>max</sub> = 440 nm, ε = 4600 M<sup>-1</sup> cm<sup>-1</sup> and a shoulder at 550 nm) is similar to that of the O-trensox bis(salicylate) complex (coordination with two arms of the ligand through the oxygen atoms of the carbonyl and hydroxyl groups) but with lower ε values. The log *K*<sub>FeLH<sub>4</sub></sub> value (3.95) is very close to that for the formation of the O-trensox bis(salicylate) complex (4.21). For the FeL species the two absorption bands at λ<sub>max</sub> = 450 nm (ε = 4600 M<sup>-1</sup> cm<sup>-1</sup>) and λ<sub>max</sub> = 590 nm (ε = 3900 M<sup>-1</sup> cm<sup>-1</sup>) are characteristic of a tris(8-hydroxyquinolate) coordination, as observed with the FeL species of the ferric O-trensox complex.<sup>[5]</sup> However, the extinction coefficient (3900 M<sup>-1</sup> cm<sup>-1</sup>) at 590 nm is lower than that measured for O-trensox (5200 M<sup>-1</sup> cm<sup>-1</sup>). The UV/Vis spectrum of the FeLH<sup>+</sup> species (λ<sub>max</sub> = 440 nm, ε = 4600 M<sup>-1</sup> cm<sup>-1</sup> and λ<sub>max</sub> = 560 nm, ε = 2900 M<sup>-1</sup> cm<sup>-1</sup>) suggests a monosalicylate, bisoxinate coordination.

As a measure of the complexing efficiency of Cox2000 for iron(III) at physiological pH, the concentration of free Fe<sup>3+</sup> under standard conditions (pH 7.4, [L]<sub>tot</sub> = 10<sup>-5</sup> M, [Fe]<sub>tot</sub> = 10<sup>-6</sup> M) expressed as pFe<sup>III</sup> (pFe<sup>III</sup> = -log [Fe<sup>3+</sup>]) is 29.1, which is very close to that of O-trensox (29.5).<sup>[5]</sup> This indicates that the substitution of the tren unit N(CH<sub>2</sub>CH<sub>2</sub>)<sub>3</sub> by the (POE)C(CH<sub>2</sub>CH<sub>2</sub>CH<sub>2</sub>)<sub>3</sub> backbone does not change the complexing efficiency of the ligand significantly.

### Hydrophilic–lipophilic balance

*Partition coefficients:* Two biphasic systems were studied for the Cox chelators (Cox200, Cox750 and Cox2000). The partition coefficients between an aqueous phase buffered at pH 7.4 (Tris buffer) and octanol or chloroform were determined (Tables 3 and 4, respectively).

Table 3. Octanol–water partition coefficients *P* for the Cox chelators and O-trensox.<sup>[a]</sup>

Entry	Ligand or Fe–Ligand	Concentration [%]				<i>P</i> <sup>[a]</sup> [%]	
		in water <sup>[b]</sup>		in octanol		at 18 h	at 96 h
		at 18 h	at 96 h	at 18 h	at 96 h	at 18 h	at 96 h
1	Cox2000	97	94	3	6	0.03	0.06
2	Cox750	57	–	43	–	<b>0.78</b>	–
3	Cox200	6	10	94	90	15.7	9.0
4	O-trensox <sup>[c]</sup>	98	–	2	–	0.02	–
5	Fe–Cox2000	99	98	1	2	0.01	0.02
6	Fe–Cox750	53	–	47	–	<b>0.90</b>	–
7	Fe–Cox200	10	–	90	–	9.0	–
8	Fe–O-trensox <sup>[c]</sup>	100	–	0	–	< 0.005	–

[a] *P* = ratio of the concentrations in water and octanol. [b] With Tris buffer. [c] Ref. [7].

Table 4. Chloroform–water partition coefficients *P*<sup>[a]</sup> of the Cox chelators and Fe–Cox complexes.

Entry	Ligand or Fe–Ligand	Concentration [%]		<i>P</i> <sup>[a]</sup>
		in water <sup>[b]</sup>	in chloroform	
9	Cox2000	1	99	99
10	Cox750	0	100	– <sup>[b]</sup>
11	Cox200	0	100	– <sup>[b]</sup>
12	Fe–Cox2000	1	99	99
13	Fe–Cox750	0	100	– <sup>[b]</sup>
14	Fe–Cox200	0	100	– <sup>[b]</sup>

[a] *P* = ratio of the concentrations in water and chloroform after 18 h. [b] In Tris buffer. [c] High *P* which could not be measured by the method employed.

The three Cox ligands and the three corresponding iron complexes constitute two interesting sets: Cox2000 and its iron complex are soluble in water and insoluble in octanol. [A long grafted POE chain can be used here instead of ionised groups (such as sulfonate in O-trensox) to obtain water solubility of the free ligand and its iron complex.] Cox200 exhibits the reverse features (water insolubility and octanol solubility). Cox750 and its iron complex are partitioned between the two phases. The narrow molecular mass distributions of POE750 and POE2000 (polydispersity indices < 1.2 measured by gel permeation chromatography) imply that this factor has only a small effect on partition coefficients.

Furthermore, the results do not vary significantly over time from 18 to 96 h (Table 3, entries 1, 3, and 5).

The linear relationship in Equation (16), where  $n$  is the stoichiometry of the complex and  $k$  is a constant representing the change in hydrophobicity when the donor groups of the ligand are moved into the iron coordination sphere of the complex, is often used to correlate the partition coefficient of the free ligand with that of the iron complex<sup>[22]</sup>.

$$\log P_{\text{complex}} = n \log P_{\text{free lig}} + k \quad (16)$$

The quite similar values of  $P_{\text{complex}}$  and  $P_{\text{free lig}}$  indicate that only the POE chain, located outside the metal coordination sphere, controls the hydrophilic–lipophilic balance. O-Trensox and its iron complex were soluble only in water; the three ionised sulfonate groups prevented solubility in octanol.

The discrepancy between the results from the two biphasic systems is most surprising: the three ligands and the three iron complexes are located entirely in the chloroform phase, despite the water solubility of Cox2000 and of its complex. This result, explained by the great affinity of the POE chains for chloroform, highlights the common misuse of partition coefficients to predict the ability of a compound to cross biological membranes: in the literature, conclusions are reached indiscriminately from results on water–octanol or water–chloroform systems! The linear relationship used by Hansch<sup>[3]</sup> ( $\log P_{\text{chloroform}} = 1.12 \log P_{\text{octanol}} - 1.34$ ) is not of general relevance.  $P$  varies dramatically with the organic phase: for example, the percentages of Fe–Cox750 in the organic phase are 4, 5, 13, 47 and 100 for ethyl acetate, cyclohexane, toluene, octanol and chloroform, respectively.

**Water–octanol–water or water–chloroform–water triphasic systems:** To mimic a transmembrane transport system, we have already reported<sup>[7]</sup> a triphasic system involving an octanol phase in contact with two separate aqueous phases A and B. The Fe<sup>III</sup> complex of the ligand (Cox750 or Cox2000) lies in the aqueous phase A, buffered at pH 7.4 (standing in for the external medium). In the second aqueous phase B (mimicking the cytosol), buffered at pH 2.2, ascorbic acid and Ferrozine® (a strong Fe<sup>II</sup>-complexing agent) were added, respectively, to reduce Fe<sup>III</sup> to Fe<sup>II</sup> and to quench Fe<sup>II</sup>. At pH 2.2, all the Fe<sup>III</sup> is complexed. The metal migrates from the source phase A to the receiving phase B across the octanolic phase and the system is not leaky. Formation of the Fe<sup>II</sup>–ferrozine complex is studied by monitoring its LMCT transition at 562 nm. The same experiments were also performed with chloroform instead of octanol (Figure 6): all the iron is transported across the organic phase, and faster transport is observed in chloroform than in octanol.

**Use of a liquid membrane: mimicking a shuttle process:** Some microorganisms involve ligand exchange for iron acquisition (a “shuttle” mechanism). In *Aeromonas hydrophila*, for example, the exchange of the iron ligand from a ferric siderophore to an iron-free siderophore bound to the receptor occurs at the cell surface.<sup>[23]</sup> This iron acquisition mechanism provides the bacterium with the ability to steal iron from

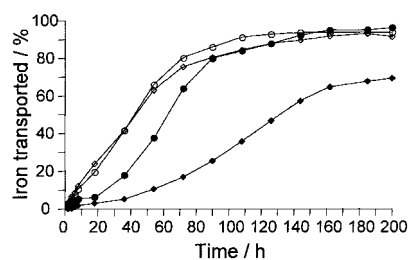


Figure 6. Percentage of iron transported per mol ligand versus time. Water–octanol–water system: phase A ( $3 \times 10^{-4}$  M): ● Cox750–Fe, ◆ Cox2000–Fe. Water–chloroform–water system: phase A ( $3 \times 10^{-4}$  M): ○ Cox750–Fe, ◇ Cox2000–Fe; phase B: [Ferozine®] =  $10^{-3}$  M, [ascorbic acid] =  $10^{-1}$  M.

exogenous siderophores. Another shuttle mechanism operates in the case of *Mycobacterium tuberculosis*, which produces two siderophores involving the same iron coordination sphere: water-soluble exochelin excreted in the external medium and lipid-soluble mycobactin. Iron is exchanged between the two siderophores (which differ only in their side chains, hydrophilic for exochelin and lipophilic for mycobactin) at the membrane surface.<sup>[24]</sup>

To mimic a shuttle system, the triphasic system described above has been used, involving an octanol or a chloroform phase containing Cox200 or Cox750 ( $10^{-6}$  M) in contact with an aqueous phase A (buffered at pH 7.4) containing Fe–edta ( $10^{-3}$  M) and an aqueous phase B (pH 2.2) containing Ferrozine® ( $10^{-4}$  M) and ascorbic acid ( $10^{-2}$  M). Formation of the Fe<sup>II</sup>–ferrozine complex was monitored as indicated above. When the experiments were carried out with octanol, iron transfer from edta to Cox200 or to Cox750 was slow (Figure 7): 35% (after 60 h) and 30% (after 120 h) of iron

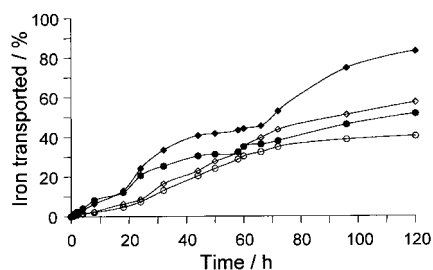


Figure 7. Percentage of iron transported per mol ligand versus time. Phase A ( $10^{-3}$  M): Fe–edta. Organic phase ( $10^{-6}$  M): ○ Cox750 in octanol, ◇ Cox200–Fe in octanol, ● Cox750–Fe in chloroform, ◆ Cox200–Fe in chloroform. Phase B: [Ferozine®] =  $10^{-4}$  M, [ascorbic acid] =  $10^{-2}$  M.

was transferred to Cox200 and Cox750, respectively. Since the initial quantity of Ferrozine® was calculated in order to quench only 50% of the iron, an excess of this compound was added after 60 h: iron transfer recommenced and, after 120 h, 60% and 40% of the metal had been transferred to Cox200 and Cox750, respectively. Similar results were obtained when chloroform was substituted for octanol (Figure 7): after 66 h 45% and 35% of iron was transferred to Cox200 and Cox750, respectively and supplementary addition of Ferrozine® led to transfer of 80% and 50% of iron.

These results feature transfer of iron across a liquid membrane through a shuttle mechanism, that is, the exchange of iron between two ligands located in the external aqueous phase and in the lipophilic phase, respectively. This system is an oversimplification, since the transport from the organic phase to the second aqueous phase is driven only by reduction of iron. The ligands Cox200 and Cox750 exhibited similar behaviour, but Cox200 had a higher efficiency in accord with the greater lipophilicity of its iron complex.

**Preliminary biological studies:** Detailed biological studies will be published elsewhere. The summary here is to allow a discussion on the physicochemical data developed in this paper.

**Plant cell nutrition:** Fe<sup>III</sup>-O-trensox was found to be able to prevent and to reverse iron chlorosis in several plant species grown in axenic conditions.<sup>[9]</sup> The use of radioactive <sup>59</sup>Fe demonstrated the incorporation of iron into ferritin, the intracellular iron storage protein. Similar studies have been started with the ferric complexes of Cox750 and Cox2000. The first results have been obtained with axenic cell cultures of *Arabidopsis thaliana*. Ferric complexes of O-trensox, Cox750 and Cox2000 were tested as the single source of iron in nutritional experiments, in which the growth and greening (iron incorporation into the chloroplasts, determined by densitometric measurements) of *A. thaliana* plant cells were compared during cell suspension cultures in axenic media. In one control experiment iron was provided with Fe<sup>III</sup>-edta, and in another no iron source was added. The ferric complexes of edta, O-trensox, Cox750 and Cox2000 led to similar kinetic results for the growth of the cells (Figures 8 and 9). These results reveal that the hydrophilic-lipophilic balance is not a deciding factor for the ability of the ferric complex to allow incorporation of iron into cells.

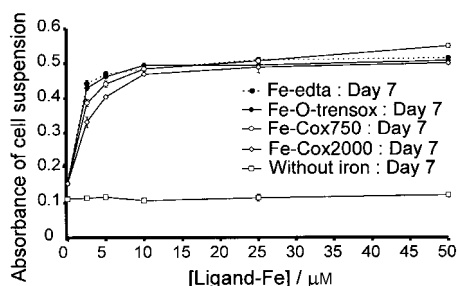


Figure 8. Greening of *A. thaliana* cells at seven days versus the concentration of the iron source: 25 °C, 220 rpm, 18 h of light per day.

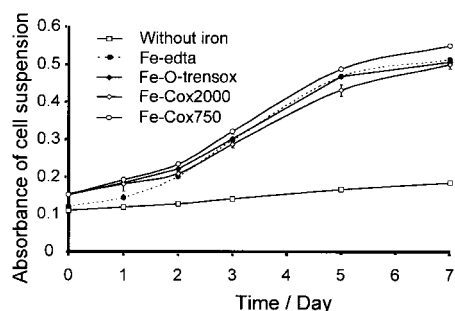


Figure 9. Greening of *A. thaliana* cells versus time: [ligand-Fe<sup>III</sup>] = 50 μM, 25 °C, 220 rpm, 18 h of light per day.

**Iron mobilisation from iron-overloaded hepatocytes:** Despite its lack of lipophilicity, O-trensox has been found to be able to mobilise iron from hepatocytes.<sup>[8]</sup> In a study of the mobilisation of iron by O-trensox, Cox2000 and Cox750 (chelator concentration 50 μM), from rat hepatocyte cultures which had been loaded in vitro with <sup>55</sup>Fe-dextran,<sup>[25]</sup> similar results were observed with both Cox2000 and Cox750, which had mobilised approximately 34% iron after 10 days (28% after two days, 30% after six days). The hydrophilic-lipophilic balance of the free chelators does not seem to be a criterion of their ability to mobilise intracellular iron.

## Conclusion

Siderophores are low molecular mass (700–1000 Da, and therefore too large to diffuse through the porin channels), Fe<sup>III</sup>-chelating compounds of microbial origin that are excreted into the environment, where they scavenge iron. Whereas the free siderophores fail to penetrate biological membranes, the ferric complexes are taken up by microbial cells by means of specific outer-membrane receptors. They traverse the membranes in energy-dependent processes and release bound iron to the cytoplasm. The release may involve reduction, ligand exchange or decomposition of the siderophore to its constituents. Biomimetic siderophores are usually envisaged as conforming with the following models<sup>[26]</sup>: 1) iron-free lipophilic carriers inhibit growth by effectively penetrating cellular membranes by diffusion, scavenging iron from intracellular stores and quitting the cells with their iron loads; 2) iron-loaded hydrophilic carriers act as growth promoters if they can introduce iron by means of iron-uptake systems.

The data reported here provide the first example of a series of iron chelators with the same pFe<sup>III</sup> and a modulated hydrophilic-lipophilic balance. We have shown that totally hydrophilic iron chelators were able to scavenge iron stored in hepatocytes with the same efficiency as iron chelators possessing the same complexing abilities but soluble in both water and organic phases. We have also shown that the ability to introduce iron into plant cells is not related to the hydrophilic-lipophilic balance of the iron complex. These results are important with regard to the criteria often claimed for biological activity of drugs, particularly iron chelators designed for chelation therapy.<sup>[22]</sup> Our results show that this cannot be a general rule and question whether the use of partition coefficients is pertinent to the prediction of the activity of iron chelators.

## Experimental Section

**Materials and methods:** Solvents were purified by the usual techniques. All other compounds were of reagent grade and were used without further purification. Iron(III) stock solutions were prepared by dissolving appropriate amounts of ferric perchlorate hydrate (Aldrich) in standardised solutions of HClO<sub>4</sub> or NaClO<sub>4</sub>. The solutions were standardised spectrophotometrically for ferric ion ( $\epsilon = 4160 \text{ M}^{-1} \text{ cm}^{-1}$  at 240 nm).<sup>[27]</sup> IR spectra were collected on a Nicolet Impact 400 spectrometer. UV/Vis absorption spectra were recorded on a Perkin-Elmer Lambda 2 spectrometer with

1.000 cm pathlength quartz cells, connected to an IBM PC 340 micro-computer. Mass spectra were recorded on a NERMAGR 101C mass spectrometer. Microanalyses were performed by the Central Service of CNRS, Solaize (France). Melting points were determined with a Büchi apparatus and are not corrected.  $^1\text{H}$  and  $^{13}\text{C}$  NMR spectra were obtained in 5 mm tubes at 25 °C with a Bruker AM 300 or AM 400 spectrometer.

#### Ligand syntheses

**Compound 1a:** A solution of tetraethylene glycol monomethyl ether (5 g, 24.03 mmol) in THF (7 mL) was added to a solution of NaOH (1.35 g, 33.65 mmol) in water (7 mL). The resulting mixture was cooled to 0 °C and a solution of tosyl chloride (4.58 g, 24.03 mmol) in THF (30 mL) was added over 2 h. The solution was stirred for an additional 2 h at 0 °C, then evaporated. The residue was dissolved in water/dichloromethane (50/100 mL); the organic layer was washed with brine and dried under  $\text{MgSO}_4$ , and the solvent was removed. The yellow residue was purified by flash chromatography (silica gel;  $\text{CH}_2\text{Cl}_2$ ). Compound **1a** was obtained as a white oil (8.1 g, 93%) pure enough for the following step. IR (film from  $\text{CHCl}_3$ ):  $\tilde{\nu}$  = 1216, 1102  $\text{cm}^{-1}$ ;  $^1\text{H}$  NMR (300 MHz,  $\text{CDCl}_3$ ):  $\delta$  = 2.45 (s, 3H;  $\text{CH}_3$ ), 3.37 (s, 3H;  $\text{CH}_2$ ), 3.52–3.70 (m, 12H;  $\text{CH}_2$ ), 3.68 (t,  $J$  = 4.9 Hz, 2H;  $\text{CH}_2$ ), 4.15 (t,  $J$  = 4.9 Hz, 2H;  $\text{CH}_2$ ), 7.36 (d,  $J$  = 8.3 Hz, 2H; ArH), 7.79 (d,  $J$  = 8.3 Hz, 2H; ArH);  $^{13}\text{C}$  NMR (75 MHz,  $\text{CDCl}_3$ ):  $\delta$  = 21.5 (CH), 58.8 (CH<sub>3</sub>), 68.5 (CH<sub>2</sub>), 69.1 (CH<sub>2</sub>), 70.35–71.8 (CH<sub>2</sub>), 127.8 (CH), 129.7 (CH), 132.9 (C<sub>q</sub>), 144.7 (C<sub>q</sub>).

**Compound 1b:** Prepared by the synthetic procedure described for **1a**, with poly(ethylene glycol) methyl ether (Acros; average  $M$  = 750, 20 g, 36.7 mmol) in THF (40 mL), NaOH (1.5 g, 37.3 mmol) in water (8 mL), and tosyl chloride (5.08 g, 26.7 mmol) in THF (60 mL). Compound **1b** was obtained as a white solid (17.6 g, 73%).  $^1\text{H}$  NMR (300 MHz,  $\text{CDCl}_3$ ):  $\delta$  = 2.45 (s, 3H;  $\text{CH}_3$ ), 3.38 (s, 3H;  $\text{CH}_2$ ), 3.58–3.71 (m, 56H;  $\text{CH}_2$ ), 4.16 (t,  $J$  = 4.8 Hz, 2H;  $\text{CH}_2$ ), 7.34 (t,  $J$  = 8.2 Hz, 2H; ArH), 7.79 (t,  $J$  = 8.2 Hz, 2H; ArH);  $^{13}\text{C}$  NMR (75 MHz,  $\text{CDCl}_3$ ):  $\delta$  = 21.5 (CH<sub>3</sub>), 58.9 (CH<sub>3</sub>), 67.3 (CH<sub>2</sub>), 68.6 (CH<sub>2</sub>), 69.1–70.6 (CH<sub>2</sub>), 71.8 (CH<sub>2</sub>), 72.4 (CH<sub>2</sub>), 127.9 (CH), 129.7 (CH), 132.9 (C<sub>q</sub>), 144.7 (C<sub>q</sub>).

**Compound 1c:** Prepared by the synthetic procedure described for **1a**, with poly(ethylene glycol) methyl ether (Aldrich; average  $M$  = 2000, 30 g, 15 mmol) in THF (60 mL), NaOH (840 mg, 21 mmol) in water (10 mL), and tosyl chloride (2.86 g, 15 mmol) in THF (40 mL). Compound **1c** was obtained as a white solid (21.97 g, 68%).  $^1\text{H}$  NMR (300 MHz,  $\text{CDCl}_3$ ):  $\delta$  = 2.44 (s, 3H;  $\text{CH}_3$ ), 3.37 (s, 3H;  $\text{CH}_2$ ), 3.4–3.8 (m, 176H;  $\text{CH}_2$ ), 4.16 (brt, 2H;  $\text{CH}_2$ ), 7.39 (t,  $J$  = 8.3 Hz, 2H; ArH), 7.80 (t,  $J$  = 8.3 Hz, 2H; ArH);  $^{13}\text{C}$  NMR (75 MHz,  $\text{CDCl}_3$ ):  $\delta$  = 21.9 (CH<sub>3</sub>), 59.4 (CH<sub>3</sub>), 69.0 (CH<sub>2</sub>), 69.6–72.3 (CH<sub>2</sub>), 72.9 (CH<sub>2</sub>), 128.0 (CH), 130.0 (CH), 132.7 (C<sub>q</sub>), 144.8 (C<sub>q</sub>).

**Compound 3a:** Sodium hydride (429 mg, 60% in paraffin) was washed with dry pentane and DMSO (5 mL) was added. A solution of **1a** in DMSO (10 mL) was added quickly and the mixture was stirred for 1 h at room temperature under a nitrogen atmosphere. A solution of **2** (3.53 g, 9.74 mmol) in DMSO (10 mL) was added over 15 min and the resulting mixture was heated to 70 °C for 18 h. The solution was evaporated and the resulting yellow oil was dissolved in chloroform, washed with brine, dried with  $\text{MgSO}_4$  and then evaporated to dryness. The white residue was purified by chromatography (silica gel; 2% MeOH in  $\text{CH}_2\text{Cl}_2$ ). Compound **3a** was obtained as a colourless oil (2.77 g, 72%) and used without further purification. IR (film from  $\text{CHCl}_3$ ):  $\tilde{\nu}$  = 2248  $\text{cm}^{-1}$ ;  $^1\text{H}$  NMR (300 MHz,  $\text{CDCl}_3$ ):  $\delta$  = 1.74 (t,  $J$  = 7.9 Hz, 6H;  $\text{CH}_2$ ), 2.42 (t,  $J$  = 7.9 Hz, 6H;  $\text{CH}_2$ ), 3.30 (s, 2H;  $\text{CH}_2$ ), 3.38 (s, 3H;  $\text{CH}_3$ ), 3.51–3.70 (m, 16H;  $\text{CH}_2$ );  $^{13}\text{C}$  NMR (75 MHz,  $\text{CDCl}_3$ ):  $\delta$  = 12.3 (CH<sub>2</sub>), 26.3 (CH<sub>2</sub>), 41.0 (C<sub>q</sub>), 59.4 (CH<sub>3</sub>), 68.5 (CH<sub>2</sub>), 69.1 (CH<sub>2</sub>), 70.3–70.6 (CH<sub>2</sub>), 71.5 (CH<sub>2</sub>), 120.0 (CN).

**Compound 3b:** Prepared by the synthetic procedure described for **3a**, by using NaH (107 mg, 2.68 mmol), **1b** (2 g, 2.2 mmol), **2** (500 mg, 2.43 mmol). Column chromatography (silica gel; 10% acetone in acetonitrile) afforded **3b** as a white oil (620 mg, 30%).  $^1\text{H}$  NMR (300 MHz,  $\text{CDCl}_3$ ):  $\delta$  = 1.74 (t,  $J$  = 8.1 Hz, 6H;  $\text{CH}_2$ ), 2.42 (t,  $J$  = 8.1 Hz, 6H;  $\text{CH}_2$ ), 3.32 (s, 2H;  $\text{CH}_2$ ), 3.38 (s, 3H;  $\text{CH}_3$ ), 3.46–3.82 (m, 68H;  $\text{CH}_2$ );  $^{13}\text{C}$  NMR (75 MHz,  $\text{CDCl}_3$ ):  $\delta$  = 12.9 (CH<sub>2</sub>), 26.6 (CH<sub>2</sub>), 40.6 (C<sub>q</sub>), 59.3 (CH<sub>3</sub>), 68.6 (CH<sub>2</sub>), 69.2 (CH<sub>2</sub>), 70.1–70.9 (CH<sub>2</sub>), 120.0 (CN).

**Compound 3c:** Prepared by the synthetic procedure described for **3a**, by using NaH (107 mg, 2.68 mmol), **1c** (4.72 g, 2.2 mmol) in DMSO (50 mL), and **2** (500 mg, 2.43 mmol). Column chromatography (silica gel; 10% acetone in acetonitrile) afforded **3c** as a white oil (1 g, 21%).  $^1\text{H}$  NMR (300 MHz,  $\text{CDCl}_3$ ):  $\delta$  = 1.68 (t,  $J$  = 8.1 Hz, 6H;  $\text{CH}_2$ ), 2.26 (t,  $J$  = 8.1 Hz,

6H;  $\text{CH}_2$ ), 3.31 (s, 2H;  $\text{CH}_2$ ), 3.39 (s, 3H;  $\text{CH}_3$ ), 3.2–3.9 (m, 170H;  $\text{CH}_2$ );  $^{13}\text{C}$  NMR (75 MHz,  $\text{CDCl}_3$ ):  $\delta$  = 12.8 (CH<sub>2</sub>), 26.2 (CH<sub>2</sub>), 40.3 (C<sub>q</sub>), 59.4 (CH<sub>3</sub>), 68.4 (CH<sub>2</sub>), 69.7–70.6 (CH<sub>2</sub>), 120.0 (CN).

**Compound 4a:** NaOH (506 mg, 12.64 mmol) and hydrazine (99%, 3 mL) were added to a solution of **3a** (1 g, 2.53 mmol) in 95% ethanol (20 mL) at 0 °C. Raney nickel (445 mg, 7.6 mmol) was added to this mixture in small portions over 2 h; the solution was stirred for an additional 6 h at room temperature. The reaction mixture was heated at reflux for 1 h, filtered hot and evaporated to give a colourless oil. Addition and evaporation of toluene were repeated until NaOH was precipitated. Evaporation of the filtrate gave **4a** as a colourless oil, which was used without further purification (938 mg, 2.3 mmol).  $^1\text{H}$  NMR (300 MHz,  $[\text{D}_6]\text{DMSO}$ ):  $\delta$  = 1.10–1.19 (m, 12H;  $\text{CH}_2$ ), 2.44 (m, 6H;  $\text{CH}_2$ ), 3.08 (s, 2H;  $\text{CH}_2$ ), 3.23 (s, 3H;  $\text{CH}_3$ ), 3.39–3.53 (m, 16H;  $\text{CH}_2$ );  $^{13}\text{C}$  NMR (75 MHz,  $[\text{D}_6]\text{DMSO}$ ):  $\delta$  = 27.1 (CH<sub>2</sub>), 31.6 (CH<sub>2</sub>), 38.1 (C<sub>q</sub>), 42.8 (CH<sub>2</sub>), 58.1 (CH<sub>3</sub>), 69.6–71.3 (CH<sub>2</sub>), 71.3 (CH<sub>2</sub>), 75.1 (CH<sub>2</sub>).

**Compound 4b:** Prepared by the synthetic procedure described for **4a**, by using NaOH (853 mg, 21.35 mmol), **3b** (1 g, 1.07 mmol) in 95% ethanol (40 mL), hydrazine 99% (5 mL) and Raney nickel (188 mg, 3.2 mmol). Compound **4b** was obtained as a colourless oil (952 mg, 1 mmol).  $^1\text{H}$  NMR (300 MHz,  $[\text{D}_6]\text{DMSO}$ ):  $\delta$  = 1.07–1.23 (m, 12H;  $\text{CH}_2$ ), 2.45 (m, 6H;  $\text{CH}_2$ ), 3.09 (s, 2H;  $\text{CH}_2$ ), 3.29 (s, 3H;  $\text{CH}_3$ ), 3.41–3.52 (m, 61H;  $\text{CH}_2$ );  $^{13}\text{C}$  NMR (75 MHz,  $[\text{D}_6]\text{DMSO}$ ):  $\delta$  = 27.1 (CH<sub>2</sub>), 31.5 (CH<sub>2</sub>), 38.1 (C<sub>q</sub>), 42.8 (CH<sub>2</sub>), 58.0 (CH<sub>3</sub>), 60.2 (CH<sub>2</sub>), 69.6–71.3 (CH<sub>2</sub>), 71.6 (CH<sub>2</sub>), 75.1 (CH<sub>2</sub>).

**Compound 4c:** Prepared by the synthetic procedure described for **4a**, by using NaOH (1.83 g, 45.72 mmol), **3c** (2 g, 0.91 mmol) in 95% ethanol (80 mL), hydrazine (99%, 10 mL), and Raney nickel (160 mg, 2.7 mmol). Compound **4b** was obtained as a colourless oil (1.91 g, 95%).  $^1\text{H}$  NMR (300 MHz,  $[\text{D}_6]\text{DMSO}$ ):  $\delta$  = 1.06–1.23 (m, 12H;  $\text{CH}_2$ ), 2.42 (brt, 6H;  $\text{CH}_2$ ), 3.08 (s, 2H;  $\text{CH}_2$ ), 3.22 (s, 3H;  $\text{CH}_3$ ), 3.34–3.59 (m, 174H;  $\text{CH}_2$ );  $^{13}\text{C}$  NMR (75 MHz,  $[\text{D}_6]\text{DMSO}$ ):  $\delta$  = 27.1 (CH<sub>2</sub>), 31.7 (CH<sub>2</sub>), 38.1 (C<sub>q</sub>), 42.7 (CH<sub>2</sub>), 58.0 (CH<sub>3</sub>), 60.9 (CH<sub>2</sub>), 69.4–71.2 (CH<sub>2</sub>), 75.1 (CH<sub>2</sub>).

**Compound 6a (Cox200):** Compound **5** (697 mg, 3.68 mmol) was dissolved in freshly distilled THF (100 mL) under nitrogen and heated at reflux. A solution of carbonyldiimidazole (656 mg, 4.05 mmol) in dry THF (50 mL) was added over 30 min. Then a solution of **4a** (0.5 g, 1.23 mmol) in dry THF (50 mL) was added over 30 min. The mixture was stirred overnight and evaporated. The resulting orange residue was dissolved in chloroform (150 mL), washed with brine, dried with  $\text{Na}_2\text{SO}_4$  and then evaporated to dryness. The residue was applied to a Sephadex LH-20 column (50% MeOH– $\text{CH}_2\text{Cl}_2$ ). An orange foam (**6a**) eluted as a single band (1.42 g, 40%). IR (film from  $\text{CHCl}_3$ ):  $\tilde{\nu}$  = 3460–3200, 1648  $\text{cm}^{-1}$ ;  $^1\text{H}$  NMR (300 MHz,  $\text{CDCl}_3$ ):  $\delta$  = 1.35 (m, 6H;  $\text{CH}_2$ ), 1.58 (m, 6H;  $\text{CH}_2$ ), 3.13 (s, 2H;  $\text{CH}_2\text{O}$ ), 3.30 (s, 3H;  $\text{CH}_3\text{O}$ ), 3.35–3.66 (m, 22H;  $\text{CH}_2$ ), 7.22 (d,  $J$  = 8.7 Hz, 3H; ArH), 7.39 (dd,  $J$  = 7.9 and 4.3 Hz, 3H; ArH), 8.03 (d,  $J$  = 7.9 Hz, 3H; ArH), 8.10 (d,  $J$  = 8.7 Hz, 3H; ArH), 8.14 (brs, 3H; NH), 8.78 (d,  $J$  = 4.3 Hz, 3H; ArH), 9.67 (brs, 3H; OH);  $^{13}\text{C}$  NMR (70 MHz,  $\text{CDCl}_3$ ):  $\delta$  = 22.9 (CH<sub>2</sub>), 31.4 (CH<sub>2</sub>), 38.5 (C<sub>q</sub>), 40.3 (CH<sub>2</sub>), 58.7 (CH<sub>3</sub>O), 70.3–71.7 (CH<sub>2</sub>), 75.03 (CH<sub>2</sub>), 113.1 (C<sub>q</sub>), 117.1 (CH), 122.9 (CH), 126.1 (CH), 130.13 (C<sub>q</sub>), 135.8 (CH), 138.8 (C<sub>q</sub>), 148.4 (CH), 154.1 (COH), 167.1 (C=O); MS (FAB, NBA matrix):  $m/z$ : 921  $[M+1]^+$ ; elemental analysis calcd (%) for  $\text{C}_{50}\text{H}_{60}\text{N}_6\text{O}_{11}$  · 0.75 MeOH · 0.25  $\text{CH}_2\text{Cl}_2$ : C 61.74, H 6.68, N 8.31; found: C 61.79, H 6.58, N 8.62.

**Compounds 6b (Cox750):** Compound **5** (600 mg, 3.16 mmol) was dissolved in freshly distilled THF (200 mL) under a nitrogen atmosphere and refluxed. Carbonyldiimidazole (564 mg, 3.48 mmol) in dry THF (20 mL) was added over 20 min, followed by a solution of **4b** (0.5 g, 0.55 mmol) in dry dichloromethane (200 mL) over 1 h. The mixture was refluxed with stirring for an additional 48 h and then evaporated. The resulting residue was applied to a Sephadex LH-20 column (50% MeOH/ $\text{CH}_2\text{Cl}_2$ ). The first fractions were evaporated and the orange-green residue was applied to a second column. Compound **6b** eluted as a single band (246 mg, 32%).  $^1\text{H}$  NMR (300 MHz,  $\text{CDCl}_3$ ):  $\delta$  = 1.32 (m, 6H;  $\text{CH}_2$ ), 1.52 (m, 6H;  $\text{CH}_2$ ), 3.01 (m, 6H;  $\text{CH}_2$ ), 3.12 (s, 2H;  $\text{CH}_2\text{O}$ ), 3.29 (s, 3H;  $\text{CH}_3\text{O}$ ), 3.37–3.60 (m, 68H;  $\text{CH}_2$ ), 7.18 (d,  $J$  = 8.8 Hz, 3H; ArH), 7.37 (m, 3H; ArH), 8.04 (m, 9H; ArH + NH), 8.73 (d,  $J$  = 4.1 Hz, 3H; ArH);  $^{13}\text{C}$  NMR (75 MHz,  $\text{CDCl}_3$ ):  $\delta$  = 23.0 (CH<sub>2</sub>), 31.5 (CH<sub>2</sub>), 38.6 (C<sub>q</sub>), 40.3 (CH<sub>2</sub>), 58.8 (CH<sub>3</sub>O), 69.8–71.8 (CH<sub>2</sub>), 75.2 (CH<sub>2</sub>), 113.4 (C<sub>q</sub>), 116.4 (CH), 122.9 (CH), 126.5 (CH), 130.1 (C<sub>q</sub>), 135.8 (CH), 138.9 (C<sub>q</sub>), 148.4 (CH), 154.5 (COH), 166.8 (C=O).



**Compound 6c (Cox2000):** Prepared according to the synthetic procedure described for **6b**, by using **5** (260 mg, 1.36 mmol) in THF (100 mL), carbonyldiimidazole (243 mg, 1.5 mmol) in THF (20 mL), and **4c** (500 mg, 0.23 mmol) in dichloromethane (200 mL). Compound **6c** was obtained as a brown solid (249 mg, 40%).  $^1\text{H NMR}$  (300 MHz,  $\text{CDCl}_3$ ):  $\delta$  = 1.32 (m, 6H;  $\text{CH}_2$ ), 1.57 (m, 6H;  $\text{CH}_2$ ), 3.17 (s, 2H;  $\text{CH}_2\text{O}$ ), 3.28 (s, 3H;  $\text{CH}_3\text{O}$ ), 3.4–3.7 (m, 185H;  $\text{CH}_2$ ), 7.25 (d,  $J$  = 8.8 Hz, 3H; ArH), 7.4 (dd,  $J$  = 8.3 and 4.2 Hz, 3H; ArH), 7.82 (brt, 3H; NH), 8.01 (d,  $J$  = 8.8 Hz, 3H; ArH), 8.07 (dd,  $J$  = 8.3 and 1.3 Hz, 3H; ArH), 8.72 (d,  $J$  = 4.2 and 1.3 Hz, 3H; ArH);  $^{13}\text{C NMR}$  (75 MHz,  $\text{CDCl}_3$ ):  $\delta$  = 23.4 ( $\text{CH}_2$ ), 32.4 ( $\text{CH}_2$ ), 39.0 ( $\text{C}_q$ ), 41.2 ( $\text{CH}_2$ ), 59.4 ( $\text{CH}_3\text{O}$ ), 69.6–72.0 ( $\text{CH}_2\text{O}$ ), 75.4 ( $\text{CH}_2$ ), 113.2 ( $\text{C}_q$ ), 117.3 (CH), 123.9 (CH), 125.9 (CH), 131.1 ( $\text{C}_q$ ), 136.3 (CH), 139.8 ( $\text{C}_q$ ), 149.2 (CH), 156.5 (COH), 168.0 (C=O).

**Fe–Cox200:** KOH (1M, 170  $\mu\text{L}$  in ethanol) was added to a solution of Cox200 (50 mg, 0.054 mmol) in methanol (10 mL) and dichloromethane (10 mL). When  $[\text{Fe}(\text{acac})_3]$  (0.054 mmol) was added, the solution instantly turned green. It was stirred for 30 min, then evaporated. The residue was applied to a Sephadex LH-20 column (50% MeOH– $\text{CH}_2\text{Cl}_2$ ). A green solid (after evaporation) eluted as a single band (49 mg, 93%). MS (FAB, NBA matrix):  $m/z$ : 974  $[\text{M}+1]^+$ .

**X-ray data collection and crystal structure determination:** Crystals of X-ray quality were obtained by vapour diffusion of diethyl oxide into a solution of the complex in methanol. The crystal of complex Fe–Cox200 was mounted on an Enraf-Nonius CAD4 diffractometer using a graphite crystal monochromator ( $\lambda(\text{MoK}\alpha) = 0.71073 \text{ \AA}$ ) at 293 K. The reflections were corrected for Lorentz and polarisation effects but not for absorption. The structure was solved by direct methods and refined using *TEXSAN* software.<sup>[28]</sup>  $[\text{FeC}_5\text{O}_7\text{H}_5\text{N}_6\text{O}_1] \cdot \text{H}_2\text{O}$ :  $M = 991.90$ , dark-green platelet (0.1  $\times$  0.2  $\times$  0.3 mm), triclinic, space group  $P\bar{1}$ ,  $a = 10.611(4)$ ,  $b = 13.129(3)$ ,  $c = 18.109(2) \text{ \AA}$ ,  $\alpha = 93.22(1)^\circ$ ,  $\beta = 101.77(2)^\circ$ ,  $\gamma = 97.51(2)^\circ$ ,  $V = 2440(1) \text{ \AA}^3$ ,  $Z = 2$ ,  $\rho = 1.350 \text{ g cm}^{-3}$ ,  $\mu = 1.081 \text{ mm}^{-1}$ , 14659 reflections collected in the range  $4^\circ \leq 2\theta \leq 60^\circ$ . All non-hydrogen atoms were refined with anisotropic thermal parameters. Hydrogen atoms were generated in idealised positions, riding on the carrier atoms, with isotropic thermal parameters, except that the hydrogen atoms of C18–24 (polyoxyethylene chain) were not generated because thermal parameters are high. Final cycle refinement, including 622 parameters, converged to  $R(F) = 0.077$  and  $R_w(F) = 0.094$  for 6135  $F > 2\sigma(F)$ ,  $S = 1.87$ ,  $\Delta\rho_{\text{max}} = 0.99 \text{ e \AA}^{-3}$ ,  $\Delta\rho_{\text{min}} = -0.46 \text{ e \AA}^{-3}$ . The two highest peaks on the difference Fourier map were localised near C22, which is in the tail of the POE chain. Crystallographic data (excluding structure factors) for the structure reported in this paper have been deposited with the Cambridge Crystallographic Data Centre as supplementary publication no. CCDC-170954. Copies of the data can be obtained free of charge on application to CCDC, 12 Union Road, Cambridge CB21EZ, UK (fax: (+44) 1223-336-033; e-mail: deposit@ccdc.cam.ac.uk).

**Potentiometric measurements:** All the measurements were made at 25 °C in deionised and twice-distilled water. The ionic strength was kept constant at 0.1M (sodium perchlorate, PROLABO, Puriss). The potentiometric titrations were performed by using a DMS Titrimo (Metrohm) automatic titrator system equipped with a combined glass electrode (Metrohm filled with saturated NaCl solution) and connected to an IBM Aptiva micro-computer. The electrodes were calibrated to read the pH according to the classical method<sup>[29]</sup> (from titration of 0.01M  $\text{HClO}_4$  with 0.01M NaOH). The ligand and its iron(III) complex (1 mM) were titrated with standardised 0.02M NaOH. Argon was bubbled through the solutions to exclude  $\text{CO}_2$  and  $\text{O}_2$ . Carbonate content was checked by Gran's method. The titration data were refined by the non-linear least-squares fitting program SUPERQUAD<sup>[16]</sup> to determine the ligand deprotonation constants.

**Spectrophotometric measurements:** The temperature was maintained at 25 °C with a Perkin–Elmer PTP-1 variable-temperature unit and the acquisition was made with UV Winlab software (Perkin–Elmer). The ionic strength was kept constant at 0.1M (sodium perchlorate). pH was measured with a 713 Metrohm digital pH meter equipped with a microelectrode. The titration of a solution containing Cox2000 and ferric ion was carried out as previously described<sup>[5]</sup> and the absorbance data were analysed using the non-linear least-squares fitting program LETAGROP-SPEFO.<sup>[18, 19]</sup> The calculations were performed by using absorbance values at 10–24 wavelengths and the residual square sums of the fit were  $10^{-3}$ – $10^{-4}$ . The spectrophotometric competition experiments were carried out with  $\text{Na}_2\text{H}_2\text{edta}$  over the pH range 2–3. Equimolar ( $10^{-4}\text{M}$ ) solutions in ferric ions,

Cox2000 and  $\text{Na}_2\text{H}_2\text{edta}$  were prepared. The samples were allowed to equilibrate for seven days at 25 °C.

**Partition coefficients and triphasic systems:** The partition coefficients between an aqueous phase buffered at pH 7.4 (Tris buffer) and octanol or chloroform were determined by a known procedure.<sup>[30]</sup> The triphasic water–octanol–water system has been described previously.<sup>[7]</sup> Phase A (2.5 mL) buffered at pH 7.4 (Tris buffer) contained a solution (0.3 mM) of the  $\text{Fe}^{\text{III}}$  complex of Cox2000 or Cox750. Phase B (8 mL, pH 2.2) contained Ferrozine® (1 mM) and ascorbic acid (0.1M). Phases A and B, which were separated by the organic phase (6 mL) of octanol or chloroform, were stirred at a constant rate at 25 °C. The time dependence of the UV/Vis spectrum of phase B (formation of the  $\text{Fe}^{\text{II}}$ –ferrozine complex) was followed by monitoring the LMCT transition at 562 nm. For the shuttle process experiments the triphasic water–octanol–water system was: phase A: 2.5 mL,  $10^{-3}\text{M}$   $\text{Fe}^{\text{III}}$ –edta, pH 7.4; phase B: 11 mL,  $10^{-4}\text{M}$  Ferrozine®,  $10^{-2}\text{M}$  ascorbic acid, pH 2.2; octanolic phase, 5.5 mL,  $10^{-6}\text{M}$  Cox200 or Cox750. After 60 h, 1 mL of a Ferrozine® solution ( $10^{-1}\text{M}$ ) was added. The triphasic water–chloroform–water system was: phase A, 2 mL,  $10^{-3}\text{M}$   $\text{Fe}^{\text{III}}$ –edta, pH 7.4; phase B, 2 mL of a Ferrozine® solution ( $10^{-4}\text{M}$ ) and ascorbic acid ( $10^{-2}\text{M}$ ), pH 2.2; chloroform phase, 4 mL,  $10^{-6}\text{M}$  Cox200 or Cox750. After 60 h, 250  $\mu\text{L}$  of a Ferrozine® solution ( $10^{-1}\text{M}$ ) was added. Phases A and B were stirred at a constant rate at 25 °C. The time dependence of UV/Vis spectrum of phase B (formation of the  $\text{Fe}^{\text{II}}$ –ferrozine complex) was followed by monitoring the MLCT transition at 562 nm.

**Plant cell nutrition:** Cell culture and growth measurements were carried out as previously described.<sup>[11]</sup> The axenic medium (MS) was prepared according to reference [31]. An iron-free control was cultivated in the iron-free nutrient solution MS. The assays were performed in MS supplemented with  $\text{Fe}^{\text{III}}$ –Cox750,  $\text{Fe}^{\text{III}}$ –Cox2000,  $\text{Fe}^{\text{III}}$ –trensox and  $\text{Fe}^{\text{III}}$ –edta, respectively, from 5 to 50  $\mu\text{M}$ , with six independent replications. Densitometric measurements were made daily as previously described.<sup>[31]</sup> The Biorad Geldoc 1000 video camera system, with “molecular analyst” software, was used for quantification. Full-frame images were captured in constant light conditions (that is, white light was adjusted so that just a few saturated pixels appeared in red in the empty optical field). A reproducible relationship was found between the absorbance of the wells in densitometric scanning profiles of recorded images and the number of cells in the wells.

## Acknowledgements

The authors thank the members of GDR CNRS 1879: R. R. Crichton, C. Henry (Université de Louvain, Belgium), J.-P. Laulhère (CEA Grenoble), and G. Lescoat and N. Rakba (Université de Rennes, France) for the biological studies mentioned in this paper and for fruitful discussions.

- [1] “Iron Transport and Storage in Microorganisms, Plants and Animals”: *Met. Ions Biol. Syst.* **1998**, 35, whole volume.
- [2] K. N. Raymond, G. Müller, B. F. Matzanke, *Top. Curr. Chem.* **1984**, 123, 49–102.
- [3] C. Hansch, *Acc. Chem. Res.* **1969**, 2, 232–239.
- [4] P. Baret, C. Béguin, H. Boukhalfa, C. Caris, J.-P. Laulhère, J.-L. Pierre, G. Serratrice, *J. Am. Chem. Soc.* **1995**, 117, 9760–9761.
- [5] G. Serratrice, H. Boukhalfa, C. Béguin, P. Baret, C. Caris, J.-L. Pierre, *Inorg. Chem.* **1997**, 36, 3898–3910.
- [6] G. Serratrice, F. Biaso, P. Baret, J.-L. Pierre, *J. Inorg. Biochem.*, in press.
- [7] F. Thomas, P. Baret, D. Imbert, J.-L. Pierre, G. Serratrice, *Bioorg. Med. Chem. Lett.* **1999**, 9, 3035–3040.
- [8] N. Rakba, F. Aouad, C. Henry, C. Caris, I. Morel, P. Baret, J.-L. Pierre, P. Brissot, R. J. Ward, G. Lescoat, R. R. Crichton, *Biochem. Pharmacol.* **1998**, 55, 1797–1806.
- [9] C. Caris, P. Baret, C. Béguin, G. Serratrice, J.-L. Pierre, J.-P. Laulhère, *Biochem. J.* **1995**, 312, 879–885.
- [10] R. J. Bergeron, J. Wiegand, J. S. Mc Manis, T. Thirumalai Perumal, *J. Med. Chem.* **1991**, 34, 3182–3187.

- [11] D. Imbert, F. Thomas, P. Baret, G. Serratrice, D. Gaude, J.-L. Pierre, J.-P. Laulhère, *New J. Chem.* **2000**, *24*, 281–288.
- [12] P. Job, *Ann. Chim.* **1927**, *9*, 113–203.
- [13] L. Pech, Y. A. Bankovsky, A. Kemme, J. Lejeijs, *Acta Crystallogr. Sect. C* **1997**, *53*, 1943–1945.
- [14] G. Serratrice, P. Baret, H. Boukhalfa, I. Gautier-Luneau, D. Luneau, J.-L. Pierre, *Inorg Chem.* **1999**, *38*, 840–841.
- [15] M. S. Cohen, M. Meyer, K. N. Raymond, *J. Am. Chem. Soc.* **1998**, *120*, 6277–6286.
- [16] T. D. P. Stack, T. B. Karpishin, K. N. Raymond, *J. Am. Chem. Soc.* **1992**, *114*, 1512–1514.
- [17] P. Gans, A. Sabatini, A. Vacca, *J. Chem. Soc. Dalton Trans.* **1985**, 1195–1200.
- [18] L. G. Sillen, B. Warsquist, *Ark. Kemi* **1969**, *31*, 377–390.
- [19] M. Meloun, J. Havel, E. Hogfeldt, *Computation of Solution Equilibria*, Ellis Horwood, Chichester, **1988**.
- [20] A. E. Martell, R. M. Smith, *Critical Stability Constants*, Plenum, New York, **1974**.
- [21] A. Ringbom, *Complexation in Analytical Chemistry*, Interscience, New York, **1963**.
- [22] J. T. Edwards, *Biometals* **1998**, *11*, 203–205.
- [23] A. Stinzi, C. Barnes, J. Xu, K. N. Raymond, *Proc. Natl. Acad. Sci. USA* **2000**, *97*, 10691–10696.
- [24] J. M. Roosenberg, Y. M. Lin, Y. Lu, M. Miller, *Curr. Med. Chem.* **2000**, *7*, 159–197.
- [25] Unpublished results.
- [26] A. Shanzer, J. Libman, *Met. Ions Biol. Syst.* **1998**, *35*, 329–354.
- [27] R. Bastian, R. Weberling, F. Palilla, *Anal. Chem.* **1956**, *28*, 459–465.
- [28] TEXSAN: Single-Crystal Structure Analysis Software, V.1.7, Molecular Structure Corporation, 3200 Research Forest Drive, The Woodlands, TX 77381 (USA), **1995**.
- [29] A. E. Martell, R. J. Motekaitis, *Determination and Use of Stability Constants*, 2nd ed., VCH, New York, **1992**.
- [30] J. E. Bollinger, J. Mague, C. J. O'Connor, W. A. Banks, D. M. Roundhill, *J. Chem. Soc. Dalton Trans.* **1995**, 1677–1688.
- [31] T. Murashige, F. Skoog, *Physiol. Plant* **1962**, *15*, 473–479.

Received: May 25, 2001

Revised: October 31, 2001 [F3288]